

Dose Distributions in a Plastic Phantom Irradiated by 40- and 65-MeV Quasi-Monoenergetic Neutrons

Y. Nakane and Y. Sakamoto
Japan Atomic Energy Research Institute, Ibaraki-ken 319-1195, Japan

ABSTRACT

Dose distributions in a plastic phantom irradiated by 40- and 65-MeV quasi-monoenergetic neutrons were measured with a tissue equivalent proportional counter. Measured distributions were compared with those calculated by using the HETC-3STEP and the MORSE-CG codes, showing good agreement between them.

INTRODUCTION

From the viewpoint of radiation protection for high energy accelerator facilities, it is important to establish an evaluation method of effective dose for high and intermediate energy radiations. The HERMES code system(1) has been extended(2) to calculate the effective dose up to 10 GeV neutrons. The accuracy of the code system, however, has not been validated experimentally for intermediate and high energy neutrons. For the validation of the code system for intermediate energy neutrons, reaction rate distributions in a slab phantom have been measured(3) by using a ^{238}U fission counter and solid state nuclear track detectors for 40- and 65-MeV quasi-monoenergetic neutrons generated from the $^7\text{Li}(p,n)$ reactions with 43- and 68-MeV protons at the AVF cyclotron facility, TIARA (Takasaki Ion Accelerators for Advanced Radiation Application) facility, of Japan Atomic Energy Research Institute. In the present work, absorbed dose distributions and microdosimetric spectra in the phantom were measured for 40- and 65-MeV quasi-monoenergetic neutrons with a tissue equivalent proportional counter (TEPC). Average quality factors and dose equivalent distributions in the phantom were obtained from the microdosimetric spectra and the $Q(y)$ relationship. The measured dose distributions were compared with the calculated ones by using the HETC-3STEP(2) and the MORSE-CG/KFA(1) codes. In addition, for an evaluation of dose contributions of neutrons below 10 MeV, the energy spectra of source neutrons were measured with using a spherical multi-moderator spectrometer, while those above 10 MeV have been measured(4) by a time of flight (TOF) method with a BC501A organic liquid scintillator.

EXPERIMENTS

Experimental Setup

Figure 1 shows a cross sectional view of the experimental arrangement at the TIARA facility. Quasi-monoenergetic source neutrons ("40 MeV" and "65 MeV") of about 40 and 65 MeV were produced in 3.6 mm and 5.2 mm thick ^7Li -targets bombarded with 43- and 68-MeV protons, respectively. Source neutrons emitted in the forward direction were introduced to a 10.9-cm-diameter and 220-cm-long iron collimator embedded in a

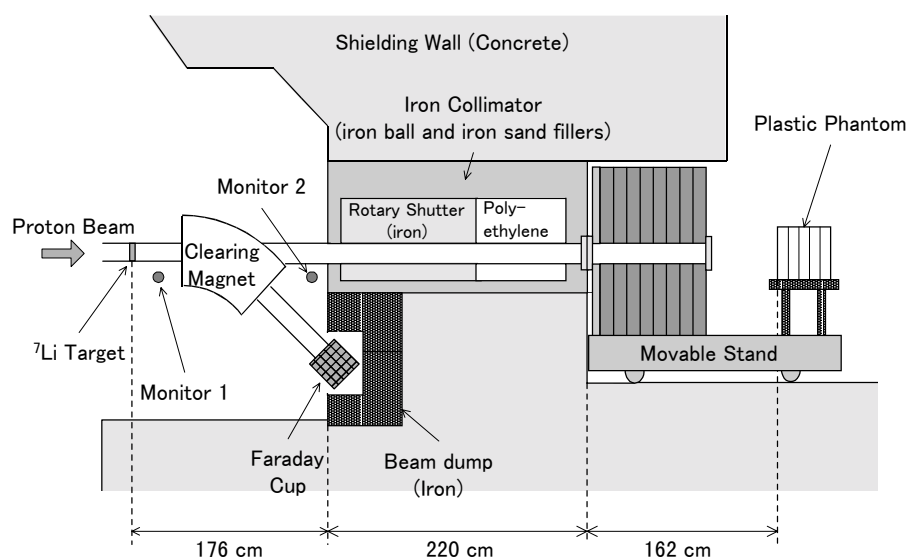


Figure 1. Cross sectional view of the experimental arrangement

shielding wall and a 10.9-cm-diameter and 85-cm-long additional collimator on a movable stand, while proton beam penetrating through the target was bent down by a clearing magnet to a Faraday cup. A copper plate of 3-mm-thick was set at the exit of the additional collimator as a neutral proton beam stopper. The 30 x 30 x 30 cm³ slab phantom made of polymethyl methacrylate was placed on the beam at the position of 558 cm from the Li target. Source neutron spectra above 10 MeV have been measured(4) by the TOF method with a 12.7-cm-diameter x 12.7-cm-long BC501A liquid scintillation detector as shown in Figure 2. The peak intensities of the source neutrons have been measured(5) by using a proton-recoil-counter-telescope (PRT). The intensity of neutrons at the irradiating position was monitored with the proton beam Faraday cup and two fission counters placed near the target and the collimator, of which efficiencies had been calibrated with the PRT. Error of neutron intensity monitoring was estimated to less than 7%. Absorbed dose and microdosimetric spectra along the center line of the phantom were measured with the tissue equivalent proportional counter (TEPC). Average quality factors and dose equivalent distribution in the phantom were obtained from the microdosimetric spectra measured by the TEPC and the quality factor, $Q(y)$, given in ICRU 40(6).

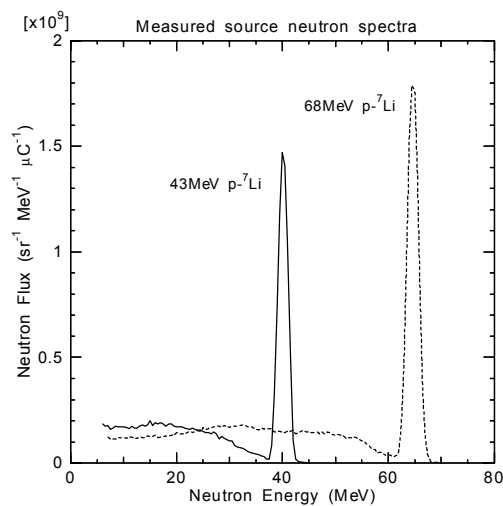


Figure 2. Measured spectra of source neutrons

Measurement of Source Neutron Spectra below 10 MeV

In the present work, the energy spectra below 10 MeV were measured with using the spherical multi-moderator spectrometer. The spectrometer consists of a 5.08-cm-diameter spherical proportional counter filled with 10 atm. ³He gas and 1.5-, 3.0-, 5.0- and 9.0-cm thicknesses of spherical polyethylene moderators. The spectrometer was set on the beam at the position of 11.90m from the Li target. In addition, the spectrometer was set at 50-cm off the beam axis to measure spectrum of background neutrons. Measured reaction rates were unfolded to the neutron energy spectra using the SAND-II code(7) with the response functions(8,9). Because of low sensitivity and similarity between the response functions of moderators in the neutron energy above 10 MeV, the contribution of reaction rate due to neutrons above 10 MeV was subtracted by using the spectrum measured by the BC501A. Using the unfolded spectra at the position of spectrometer measurements, source neutron spectra at the Li target position were calculated with the MCNP-4B code(10) and a cross section data from the LA150 library(11) processed with NJOY94(12). Almost all configurations of the wall collimator such as iron and polyethylene collimators, rotary shutter, vacuum window of 2-mm-thick stainless steel, air and the copper plate were considered in the three-dimensional calculation geometry. Finally, source neutron spectra from thermal to peak energy region at the front surface of the phantom were calculated. Calculated spectra are shown in Figure 3.

CALCULATIONS AND DISCUSSIONS

Absorbed Dose

Absorbed dose distributions in the phantom were calculated by using the code system given below. The absorbed dose caused by neutrons above 15 MeV was obtained from the deposition energy of charged particles from induced reactions calculated by the HETC-3STEP code, while that below 15 MeV was obtained from the Kerma factor given in ICRU 26(13) and neutron energy spectra calculated by the MORSE-CG/KFA code with a multi-group cross section library processed from JENDL-3(14). For comparison, the absorbed dose was also obtained for the whole energy region of neutrons from the Kerma factor and neutron energy spectra calculated by the MORSE-CG code with the DLC-119/HILO86(15) multi-group cross section library up

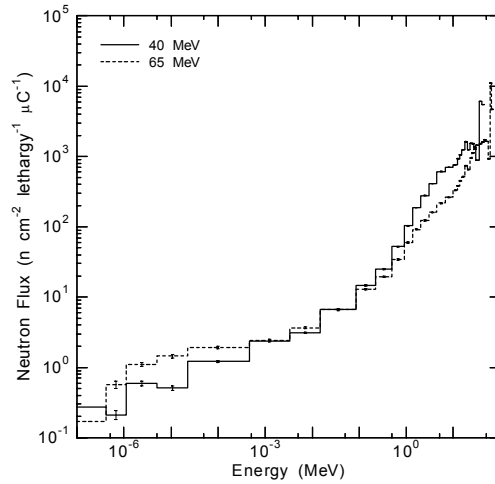


Figure 3. Calculated energy spectra of source neutrons at the front surface of the phantom

to 400 MeV. Figure 4 shows the results of measured and calculated absorbed dose distributions in the phantom. The calculated results of absorbed dose for the “40MeV” and the “65MeV” source neutrons by HETC-3STEP/MORSE-CG agree well with the experimental values within the error of 10% except for the value at the depth of 25 cm for the “40MeV” source neutron. With regard to absorbed dose distributions calculated for the whole energy region of neutrons by the MORSE-CG code, calculated results in the phantom are in good agreement with the experimental ones within 13% even at the depth of 25cm, while those on the surface of the phantom are 38% and 60% higher than the measured ones for the “40MeV” and the “65MeV” source neutrons, respectively. These disagreements are ascribed to the Kerma approximation, in which the charged particles and recoil nuclide are assumed to lose the energy closely near the reaction point.

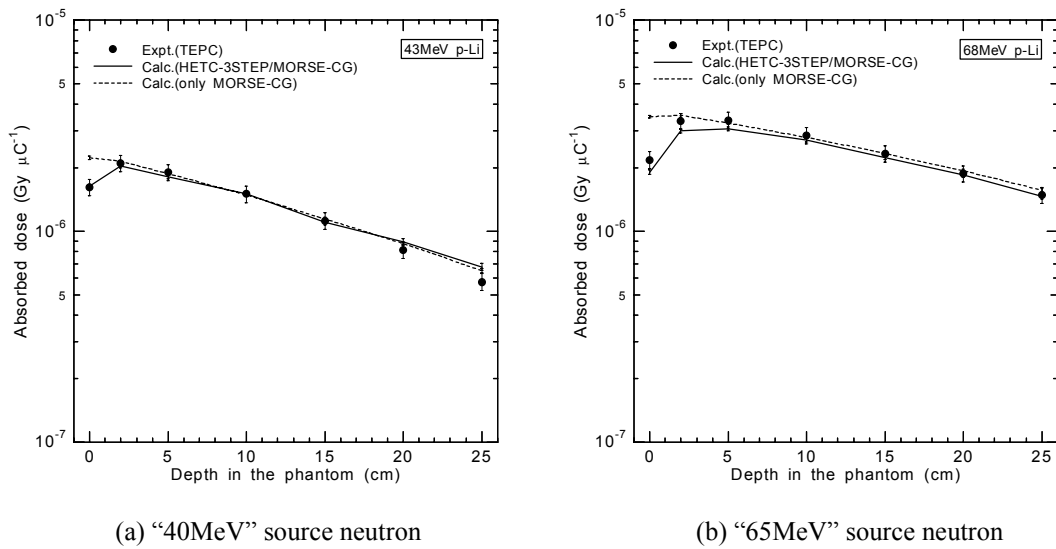


Figure 4. Measured and calculated absorbed dose distributions in the phantom

Dose Equivalent

Average quality factors and dose equivalent caused by neutrons above 15 MeV were obtained from absorbed dose spectra calculated by the HETC-3STEP code and the quality factor $Q(L)$ which was assumed to be the $Q(y)$ given in ICRU 40, while those below 15 MeV were obtained from the Kerma factor weighted by average quality factor of charged particle generated by nuclear reaction in the phantom and neutron energy spectra calculated by the MORSE-CG code. Average quality factors calculated for the “40MeV” and the “65MeV” source neutrons by HETC-3STEP/MORSE-CG agree with the measured ones within 16%. Figure 5 shows the results of measured and calculated dose equivalent distributions in the phantom. Calculated results

of dose equivalent for the “40MeV” and the “65MeV” source neutrons agree with the measured ones within 18% and 21%, respectively. Calculated average quality factor is about 15% lower than the measured one, when the absorbed dose agrees within 5%. This discrepancy can be attributed to the difference between lineal energy spectra in the experiment and the spectra of unrestricted linear energy transfer in the calculation.

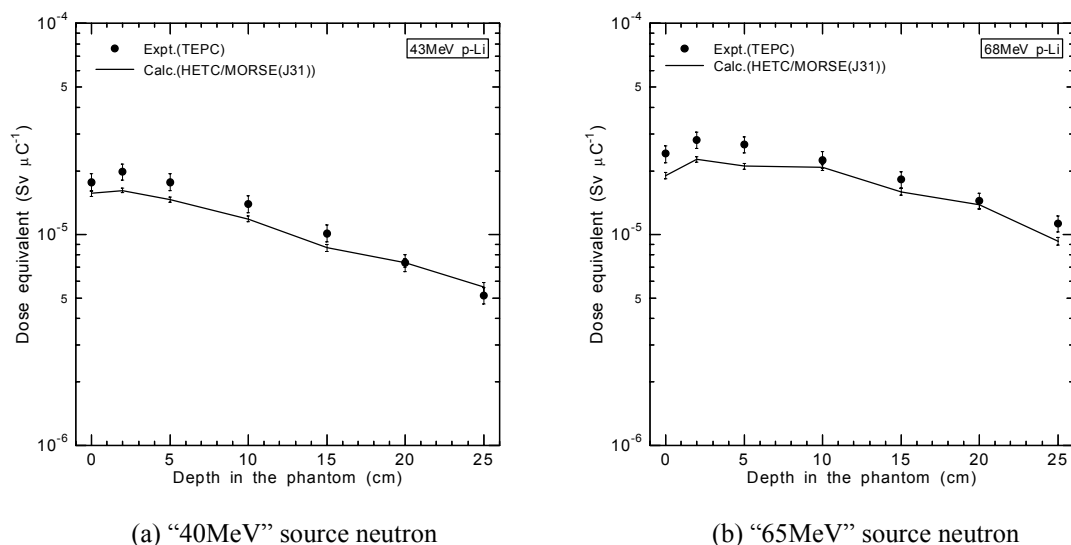


Figure 5. Measured and calculated dose equivalent distributions in the phantom

CONCLUSION

Absorbed dose and microdosimetric spectra in the plastic phantom were measured with the TEPC for 40- and 65-MeV quasi-monoenergetic neutrons. Average quality factors and dose equivalent distribution in the phantom were obtained from microdosimetric spectra measured by TEPC and the $Q(y)$ relationship. Good agreement was obtained between the measured results of the absorbed dose and the calculated ones from the deposition energy of charged particles from induced reactions by the HETC-3STEP code for the neutron energy above 15MeV and those from the Kerma factor and neutron energy spectra calculated by the MORSE-CG code for the energy below 15MeV. The results of absorbed dose obtained for the whole energy region of neutrons from neutron energy spectra calculated by the MORSE-CG code and the Kerma factor also agree well with the measured ones in the phantom, while those on the surface of the phantom are higher than the measured ones because of applying Kerma approximation to intermediate energy neutrons. Calculated results of average quality factors and dose equivalent agree with the measured ones within 16% and 21%, respectively. The discrepancy between measured and calculated results for average quality factor and dose equivalent is larger than that for absorbed dose. This can be attributed to the difference between lineal energy spectra in the experiment and the spectra of unrestricted linear energy transfer in the calculation.

REFERENCES

1. P. Cloth, D. Filges, R.D. Neef, G. Sterzenbach, Ch. Reul, T.W. Armstrong, B.L. Colborn, B. Anders and H. Bruckmann, KFA-IRE-EAN 12/88 (1988).
2. N. Yoshizawa, K. Ishibashi and H. Takada, *Development of High Energy Transport Code HETC-3STEP Applicable to the Nuclear Reaction with Incident Energies above 20 MeV*. J. Nucl. Sci. Technol. 32, 601-607 (1995).
3. Y. Nakane, H. Nakashima, Y. Sakamoto and S. Tanaka, *Measurement of Reaction Rate Distributions in a Plastic Phantom Irradiated by 40- and 65-MeV Quasi-monoenergetic Neutrons*. Radiat. Meas. 28, 479-482 (1997).
4. N. Nakao, H. Nakashima, T. Nakamura, Sh. Tanaka, Su. Tanaka, K. Shin, M. Baba, Y. Sakamoto and Y. Nakane, *Transmission Through Shields of Quasi-Monoenergetic Neutrons Generated by 43- and 68-MeV Protons- I: Concrete Shielding Experiment and Calculation for Practical Application*. Nucl. Sci. Eng. 124, 228-242 (1996).
5. M. Baba, Y. Nauchi, T. Iwasaki, T. Kiyosumi, M. Yoshioka, S. Matsuyama, N. Hirakawa, T. Nakamura, Su. Tanaka, S. Meigo, H. Nakashima, Sh. Tanaka and N. Nakao, *Characterization of a 40-90 MeV ${}^7\text{Li}(p,n)$ Neutron Source at TIARA Using a Proton Recoil Telescope and a TOF Method*. Nucl. Instrum. Methods Phys. Res. A 428, 454-465 (1999).
6. International Commission on Radiation Units and Measurements, *The Quality Factor in Radiation*

- Protection*. ICRU Report 40 (1986).
7. W.N. McElroy, S. Berg, T. Crockett and R.G. Hawkins, *A Computer Automated Iterative Method for Neutron Flux Spectra Determination by Foil Activation*, AFWL-TR-67-41. Vols. 1 through 4, Air Force Weapons Laboratory (1967).
 8. Y. Uwamino, T. Nakamura and A. Hara, *Two Types of Multi-Moderator Neutron Spectrometers: Gamma-Ray Insensitive Type and High-Efficiency Type*. Nucl. Instr. Meth., A239, 299-309 (1985).
 9. T. Ishikawa, Y. Miyama and T. Nakamura, *Neutron Penetration through Iron and Concrete Shields with the Use of 22.0- and 32.5-MeV Quasi-Monoenergetic Sources*. Nucl. Sci. Eng., 116, 278-290 (1994).
 10. J.F. Briesmeister (Editor), *MCNP - A General Monte Carlo n-Particle Transport Code, Version 4B*. LA-12625-M, Los Alamos National Laboratory (1997).
 11. M.B. Chadwick, P.G. Young, S. Chiba, S.C. Frankle, G.M. Hale, H.G. Hughes, A.J. Koning, R.C. Little, R.E. MacFarlane, R.E. Prael and L.S. Waters, *Cross Section Evaluations to 150 MeV for Accelerator-Driven Systems and Implementation in MCNPX*. Nucl. Sci. Eng., 131, 293-328 (1999).
 12. R.E. MacFarlane and D.W. Muir, *The NJOY Nuclear Data Processing System, Version 91*. LA-12740-M, Los Alamos National Laboratory (1994).
 13. International Commission on Radiation Units and Measurements, *Neutron Dosimetry for Biology and Medicine*. ICRU Report 26 (1977).
 14. K. Shibata et al., *Japanese Evaluated Nuclear Data Library, Version 3, - JENDL-3 -*. JAERI 1319 (1990).
 15. R.G. Alsmiller, J.M. Barnes and J.D. Drischler, *Neutron-Photon Multigroup Cross Sections for Neutron Energies \square 400 MeV (Revision 1)*. ORNL/TM-9801 (1986).